ORAL REFERENCE: ICF100460OR

Stress Analysis near Crack Tip in Mixed-Mode Condition by Speckle Photography Using an Intelligent Hybrid Method

Kenji Machida [1], Kenji Usui [1] and Hiroyuki Okamura [1]

[1] Department of Mechanical Engineering, Science University of Tokyo,
2641 Yamazaki, Noda-shi, Chiba, 2788510, Japan

ABSTRACT

An experiment was conducted on the compact normal and shear specimen made of homogeneous and dissimilar materials subjected to various kinds of mixed-mode loading. The displacement at any point on the specimen was obtained by pointwise filtering of the specklegram using a thin laser beam. The displacement obtained by speckle photography is not as smooth as that obtained by the finite element analysis. Therefore, the displacement data were smoothed by 2 D FFT filtering and least squares method. Then, stress-intensity factors of the asymptotic solution derived by Sun and Jih were estimated using the displacement data obtained from speckle photography by the least squares method. The displacement of each node was calculated from the asymptotic solution by using stress-intensity factors obtained by the previous process. From the nodal displacement, the stress-strain analysis was conducted by using the latter half of FEM algorithm. Moreover, the stress analysis was carried out using an intelligent hybrid method proposed by Nishioka et al. The contour diagrams of stress and strain obtained by using the raw displacement data of experiment remarkably differed from those obtained by FEM analysis. However, the stresses obtained the present analyzing system were very similar to those obtained by FEM. Consequently, the stresses near the crack tip of homogeneous and dissimilar materials can be evaluated by the present stress-analyzing system.

KEYWORDS

Stress Analysis, Stress Intensity Factor, Finite Element Analysis, Speckle Photography, 2 D Fast Fourier Transform, Young's fringes, Image Processing, Intelligent Hybrid Method

INTRODUCTION

A large amount of displacement data must be taken to investigate the singular field near the crack tip. The Young's fringes analysis procedure is usually time-consuming and tedious. Therefore, image processing is indispensable to carry out fringe analysis with high speed and accuracy. We presented an image-processing system [1][2] for the numerical processing of the diffraction pattern of Young's fringes from a double-exposure speckle photograph. The fringe spacing and orientation are determined using only one Young's fringes pattern without any other diffraction halo patterns. This system is based on the 2 D FFT and iteration using the bounded Newton-Raphson algorithm of the fringe pattern with the resolution of 256x256x8 bits. Therefore, it enables us to automatically analyze the specklegrams of a noisy and poor fringe pattern. The measurement of deformation using laser speckle photography can be carried out with high accuracy, reliability and speed. To date, the stress-intensity factors of homogeneous and dissimilar

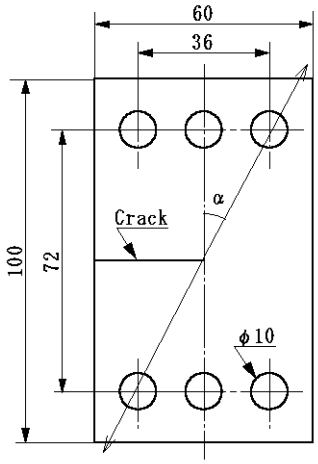

Figure 1: Specimen configuration

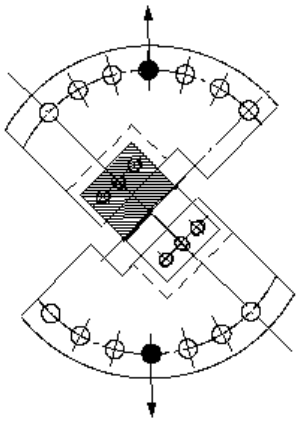

Figure 2: Loading device

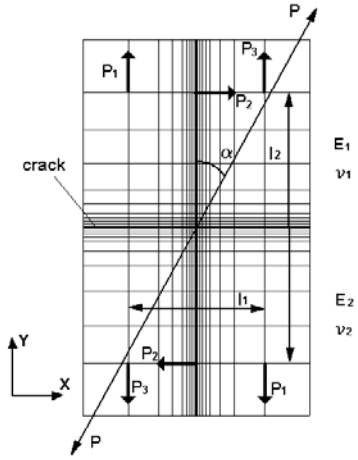

Figure 3: Mesh pattern and loading condition

materials have been evaluated with high accuracy by measuring the displacement along the crack-line on the specklegram [3]-[5]. In this study, the displacements near the crack tip of the homogeneous and dissimilar material CNS (compact normal and shear) specimens subjected to the mixed-mode loading was measured by the speckle photography. By setting up the mesh pattern similar to that in the finite-element analysis, the displacement of each nodal point was measured. The displacement data were smoothed by the 2 D FFT filtering and least squares methods. Then, stress-intensity factors of the asymptotic solution derived by Sun and Jih [6] were evaluated using the displacement data obtained from speckle photography by the least squares method. The displacement of each node was calculated from the asymptotic solution using stress-intensity factors obtained by the previous process. From the nodal displacement, the stress-strain analysis was conducted by using the latter algorithm of FEM. Finally, the stress-strain relationship was discussed in terms of comparison between the speckle photography and finite-element analysis. Moreover, the intelligent hybrid method proposed by Nishioka et al. [7][8] was applied to the stress analysis.

SMOOTHING OF DISPLACEMENT DATA

The displacement data obtained using speckle photography show so little scattering that the error must be removed. Thus, the smoothing process was carried out on the displacement components (u, v) in the x and y directions. Two smoothing methods were employed. One was the masking method using the 2 D FFT. Another was the line-smoothing method using the least squares method. In conventional image processing, the smoothing is carried out by removing the high-frequency component in the FFT. However, even the main data are destroyed in the case of small pixel data. Therefore, the frequency components were omitted except on the main axes. This method enables us to remove the large error without destroying the main data. A 2 D FFT of 4x4 displacement data was carried out, and then a 2 D inverse FFT was carried out by setting the real and imaginary parts of the low power spectrum at zero. This filtering process was performed by moving the mask step-by-step from the left to the right, and then was performed downward in turn. This process was carried out by moving the mask over all data one to four times. The protruding data were removed without destroying the main frame by this process. A small error of data on the mesh line was removed by the polynomial approximation of the least squares method. In addition, the lost data can be complemented using the least squares method during image processing.

EXPERIMENT

The two kinds of specimens that were made of the acrylic homogeneous and acrylic-aluminum dissimilar materials were used for the measurement of displacement around the crack-tip. Young's modulus and Poisson’s ratio of aluminum and acrylic resin were 67.3GPa, 0.33 and 3.06GPa, 0.38, respectively. The

configuration of specimen is shown in Fig. 1. The thickness of homogeneous and dissimilar materials was 16 mm and 15 mm, respectively. First, the upper and lower parts of the specimen were machined separately and then two pieces were bonded. A crack was introduced by introducing a Teflon sheet of 0.02 mm thickness between the two pieces during bonding. The mixed-mode loading was applied to the specimen using a device proposed by Richard and Benitz [9] as shown in Fig. 2. This device enables us to carry out the experiments under the seven kinds of mixed-mode loading. The displacement at any point on the specimen was obtained by pointwise filtering of the specklegram using a thin laser beam. For a full field analysis, the specklegram was mounted on an X-Y stage driven by stepping motors controlled by microcomputer. The displacement data were taken in the area of 10 mm(H) x12.8 mm(W) around the crack tip.

MODEL FOR ANALYSIS

The 3 D FEM model was generated by developing the 2 D mesh as shown in Fig. 3 to the thickness direction. One-half portion of the specimen was modeled by the symmetry with respect to the midsection of the specimen by using the isoparametric elements of 20 nodes. The layer division ratio was 1:2:3:4:5 from the free surface and number of elements and nodes was 2400 and 11969, respectively. The same loading condition as Kishimoto et al. [10] was employed for the mixed-mode loading. The materials 1 and 2 denote the upper and lower parts of the specimen, respectively. The homogeneous material is an acrylic resin. The material 1 is aluminum and material 2 is acrylic resin for the dissimilar material. The stress-intensity factor was evaluated by the virtual crack extension method (VCEM).

RESULTS AND DISCUSSIONS

Comparison between stress-intensity factors

To simplify the comparison between stress-intensity factors, the non-dimensional stress-intensity factors was evaluated as follows:

$$F_j = \frac{K_j}{\frac{P}{WB}\sqrt{\pi a}} \qquad (j = I, II) \tag{1}$$

Here, P is the load, W and B are the width and thickness of the specimen, respectively.
Figure 6 shows the variation of the stress-intensity factors by the experiment and FEM with a load application angle α of acrylic homogeneous material (a) and acrylic-aluminum dissimilar material interface

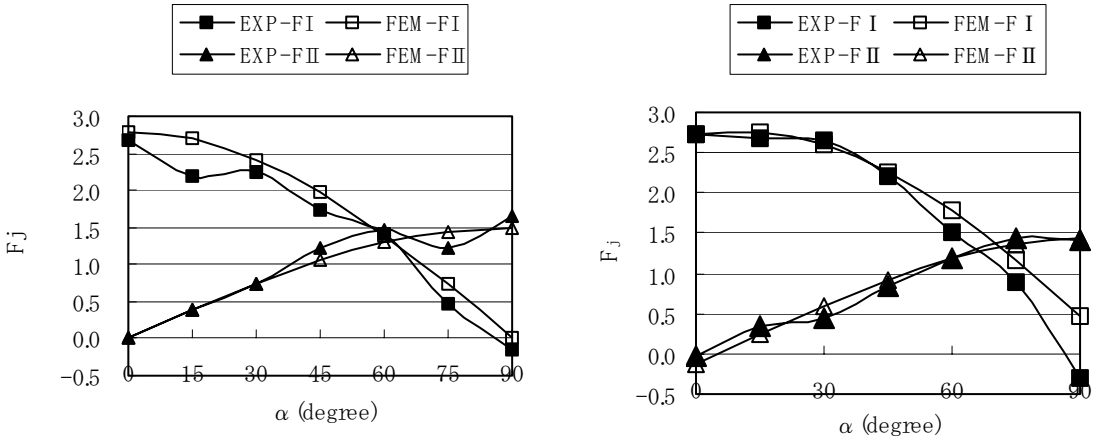

(a) Homogeneous material (b) Dissimilar material

Figure 6: Variation of stress-intensity factors with a load application angle α.

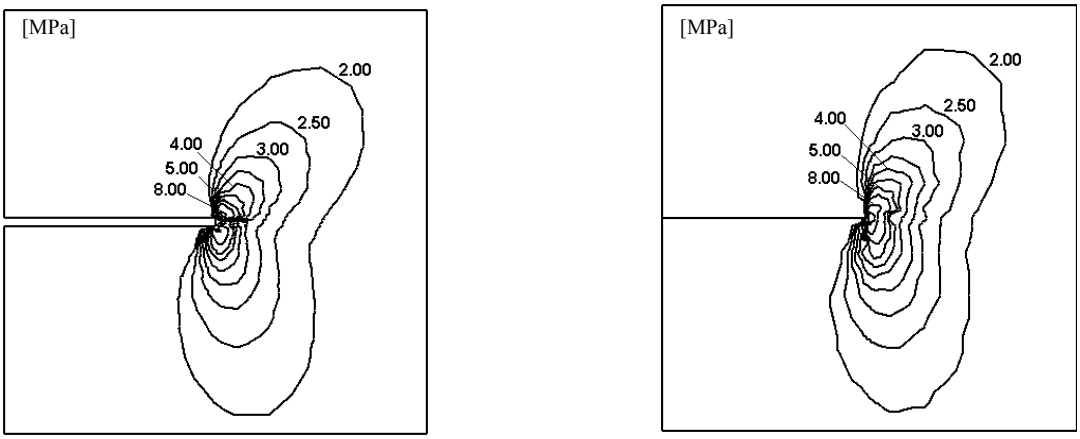

(a) EXP (b) FEM

Figure 7: Contour map of σ_y (Homogeneous)

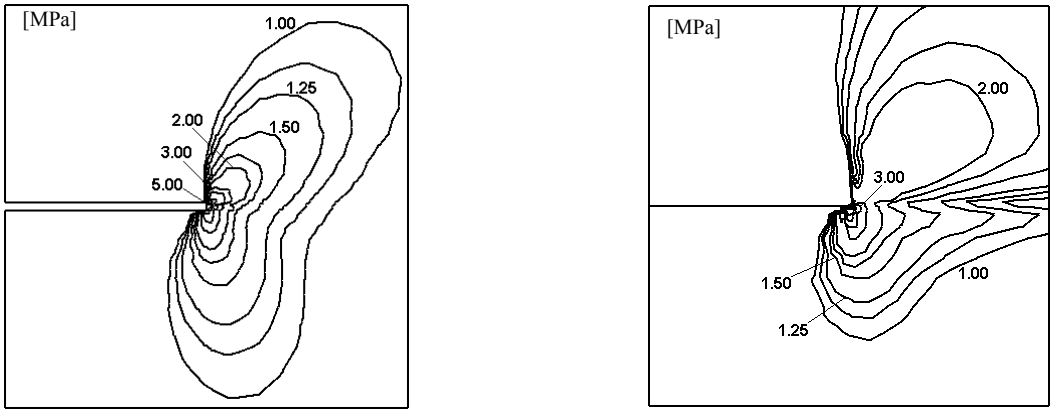

(a) EXP (b) FEM

Figure 8: Contour map of σ_y at free surface (Dissimilar)

crack (b). Although some scatter can be seen, F_I decreases while F_{II} increases with an increase in α. This tendency can be seen in both experiment and FEM. However, at α= 90 degrees, F_I showed zero or less in homogeneous material, and the large difference is seen in F_I of dissimilar material. It is considered that the same loading condition as FEM could not be performed in the experiment.

Contour map of σ_y

Figure 7 shows the contour map of σ_y (normal stress in the y direction) within 5 mm(W)x5 mm(H) at the free surface and α=45 degrees of homogeneous material. Figures 7a and 7b were obtained from the experiment which assumed the plane stress and FEM, respectively. Although the stress state of the experiment is slightly lower than that of FEM, the similar distribution can be seen in the experiment and FEM. Moreover, similar tendency was seen in the distribution of σ_x and τ_{xy}.

Figure 8 shows the contour map of σ_y at the free surface obtained by the experiment assumed a plane stress(a) and FEM (b) at α=45 degrees of dissimilar material. The upper and lower parts of this figure are aluminum and acrylic resin, respectively. Although the stress-intensity factors were nearly close, both contour map of σ_y are quite different in the dissimilar material. The stress in the experiment was calculated by the 2 D approximation assuming the plane stress or plane strain condition. However, both of the results differed from FEM. On the other hand, the 3 D analysis was carried out in FEM as mentioned above. The difference in a material constant between material 1 and material 2 causes the large difference of the displacement of the thickness direction. This is considered to have affected the stress distribution in FEM greatly.

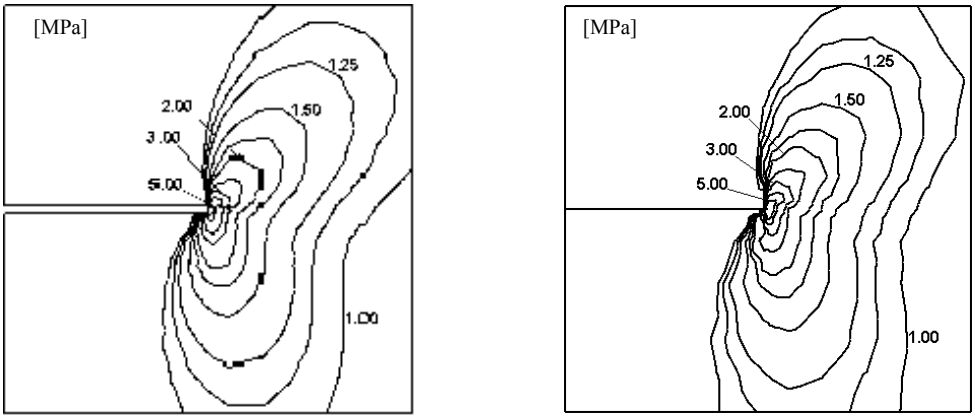

(a) EXP (Plane strain) (b) FEM (Midsection)

Figure 9: Contour map of σ_y (Dissimilar)

Figure 9 shows the contour map of σ_y at α=45 degrees of dissimilar material. Figure 9a is a contour map at the free surface obtained from the experiment by assuming the plane strain. Figure 9b is a contour map at the central part of the specimen obtained from FEM. K_I and K_{II} at the free surface assuming the plane strain were about 24% and 10% higher than those at the central part of the specimen, respectively. Although the stress value of Fig. 9a is slightly low, the shape of distribution is very similar to that of FEM (Fig. 9b). Therefore, it was revealed that the asymptotic solution of Sun and Jih is applicable to evaluate the stress field from the surface to the inside in homogeneous material and the inside except the surface in dissimilar material.

Intelligent hybrid method

The intelligent hybrid method proposed by Nishioka et al. was applied to the analysis of stress-strain from the displacement data obtained by speckle photography. Figure 10 shows the contour map of σ_y obtained from raw displacement data (a) and intelligent hybrid method (b) at the surface and α=45 degrees of homogeneous material. The raw data obtained from speckle photography were smoothed by the 2 D FFT filtering and least squares methods. However, it is difficult to evaluate the stress-strain accurately using the raw displacement data as shown in Fig. 10a. The experimental displacement field contains measurement errors so that one obtains the following finite element equation:

$$[K]\{Q^{\mathrm{mod}}\} = \{F\} - [K]\{Q^{\exp}\} \tag{2}$$

where $\{Q^{\mathrm{mod}}\}$ and $\{Q^{\exp}\}$ are the nodal displacement vectors of the modifying and experiment fields in entire hybrid analysis area. $[K]$ and $\{F\}$ are the global stiffness matrix and the global nodal force vectors, respectively. First, we calculate the following equation.

$$\{R\} = \{F\} - [K]\{Q^{\exp}\} \neq 0 \tag{3}$$

where $\{R\}$ is the restoration forces. The modifying displacement field can be evaluated by solving the following equation.

$$[K]\{Q^{\mathrm{mod}}\} = \{R\} \tag{4}$$

$\{Q^{\mathrm{mod}}\}$ can be obtained from 2 D FEM by putting R as the nodal load and constraining all nodes at the outer boundary in x and y directions. Finally, the true displacement field is obtained by the following equation.

$$\{Q\} = \{Q^{\exp}\} + \{Q^{\mathrm{mod}}\} \tag{5}$$

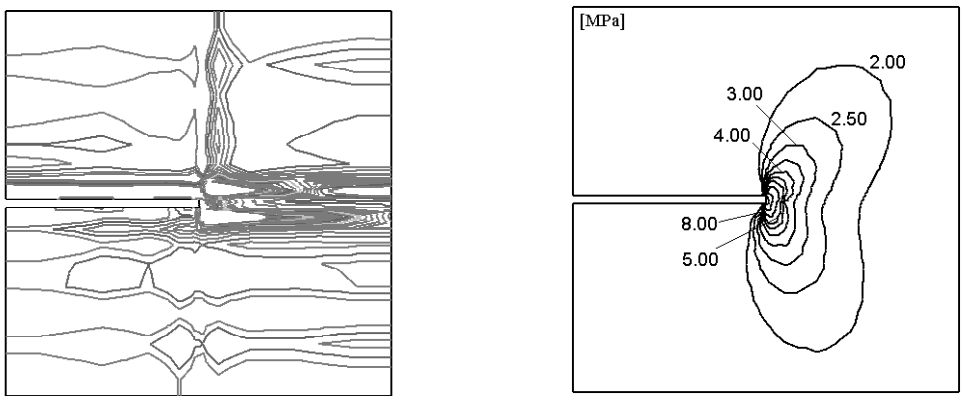

(a) Raw data (b) Hybrid method

Figure 10: Contour map of σ_y. (Homogeneous)

Figure 10a and 10b show the contour maps of σ_y obtained using raw data and hybrid method at the free surface and α=45 degrees of homogeneous material, respectively. Figure 10a shows the damaged stress distribution while Fig. 10b shows the quite similar distribution to that obtained by FEM.
The stress-strain near the crack-tip was evaluated by two methods; the asymptotic solution derived by Sun-Jih and the intelligent hybrid method. The asymptotic solution is not applicable to the general problem while the hybrid method is applicable to all problems. Therefore, the hybrid method is very useful to the stress analyzing system by experiment.

CONCLUSION

(1) The stress-intensity factors of Sun and Jih can be evaluated with high accuracy using speckle photography.
(2) The asymptotic solution derived by Sun and Jih can evaluate the stress-strain of homogeneous material with high accuracy.
(3) The intelligent hybrid method can be applied to the displacement measurement and stress-strain analysis of speckle photography.
(4) Although the asymptotic solution of Sun and Jih cannot evaluate the stress-strain of the surface of dissimilar material with an interface crack, it is applicable to stress field of the inside except the surface.

ACKNOWLEDGEMENT

The author wishes to thank Prof. Toshihisa Nishioka for his very helpful suggestion about intelligent hybrid method.

References

1. Machida, K. Kikuchi, M. Sawa, Y. and Chiang, F.P. (1994) *Trans. Jpn. Soc. Mech. Eng*., 60-573A, 1294.
2. Machida, K. Kikuchi, M. Sawa Y. and Chiang, F.P. (1994) *Optics and Lasers in Engineering,* 21-3, 151.
3. Machida, K. (1997) *OPTICAL REVIEW*, 4-2, 253.
4. Machida, K. (1997) *Trans. Jpn. Soc. Mech. Eng*., 63-6060A, 308.
5. Machida, K. (1998) *Trans. Jpn. Soc. Mech. Eng*., 64-618A, 284.
6. Sun, C.T. and Jih, C.J. (1987) *Eng. Fract. Mech*. 28-1, 13.
7. Nishioka, T. Ikekita, H. and Tamai, K. (1997), *Comp. Mech*., 20, 101.
8. Nishioka, T. Kurio, K. and Nakabayashi, H. (2000), *Exp. Mech*., 40-2, 170.
9. Richard, H.A. and Benitz, K. (1983) *Int. J. Fract*. 22, R55.
10. Kishimoto, K. Fukano, H. Yoshida, T. and Aoki, S. (1990) *Trans. Jpn. Soc. Mech. Eng*., 56-524, 957.